International Journal of Innovative
Computing, Information and Control
Volume **8**, Number **12**, December **2012**

ICIC International ©2012 ISSN 1349-4198
pp. 8399–8413

ROBUST FACIAL RECOGNITION BASED ON LOCAL GAUSSIAN STRUCTURAL PATTERN

Jorge A. Rojas Castillo, Adin Ramirez Rivera and Oksam Chae

Department of Computer Engineering
Kyung Hee University
1 Seocheon-dong, Giheung-gu, Yongin-si, Gyeonggi-do 446-701, South Korea
{ jarc; adin; oschae }@khu.ac.kr

Received October 2011; revised March 2012

Abstract. *In this paper, we propose a novel local feature descriptor, Local Gaussian Structural Pattern (LGSP), for face recognition that encodes the directional information of the face's textures (i.e., the texture's structure), producing a more discriminant code than other state-of-the-art methods. Each micro-pattern's structure is computed by using a derivative-Gaussian compass mask, which is more robust against challenging illumination and noisy conditions, and encoded by using the principal directions. Consequently, the compass mask helps distinguishing among similar structural patterns. Moreover, our descriptor encodes more information by using different resolutions of the compass mask. Thus to process a face, we divide it into several regions and extract the distribution of the LGSP features from them. Then, we concatenate these features into a feature vector, and we use it as face descriptor. We perform several experiments in which our descriptor showed consistent results under age, illumination, expression, and noise variations.*
Keywords: Image representation, Face recognition, Features extraction, Face descriptor, Local binary patter, Local directional pattern, Local Gaussian structural pattern

1. **Introduction.** Face recognition has received a great deal of attention from the scientific and industrial communities over the past decades owing to its wide range of applications in information security and access control, law enforcement, surveillance, and more generally image understanding [1]. In addition, face recognition does not require the cooperation of the individuals to be recognized. Therefore, it is a more acceptable tool despite the existence of other bio-metrics recognition approaches such as iris scans or fingerprint analysis.

We classify the face recognition descriptors into two classes according to their features into global and local. The global-feature descriptors are also called holistic methods. These methods treat the face as a whole, and extract a descriptor from it in such a way. Researches have proposed numerous approaches using the global features. In this category are Eigenfaces [2, 3], Fisherfaces [4], Laplacianfaces [5], Nearest Features Line-based Subspace Analysis [6], Neural Networks [7, 8], Wavelets [9], Fast Independent Component Analysis (ICA) [10] and kernel methods [11]. Also, different frequency features, e.g., dominant frequency features [12] and polar frequency features [13], are also analyzed for holistic face recognition. A method was proposed to extract features by employing discrete cosine transform (DCT) and Gabor wavelets, and then fused their independent features which are extracted with ICA, and Principal Component Analysis [14]. Most of these methods were initially developed with face images collected under relatively well controlled conditions. However, in practice, they have problems dealing with the different appearance variations that commonly occur in unconstrained and natural images due to pose, aging, facial expression, partial occlusions, and illumination variation. Another

problem of automatic face recognition is that facial features have limited distinctive information for personal identification and these features are genetically dependent, which means that genetically identical twins have very similar features.

Although these methods have been studied widely, local descriptors have gained attention because of their robustness to illumination and pose variation. Heisele et al. [15] showed the validity of the component based methods, and showed how they outperform holistic methods. The local feature methods compute the descriptor form parts of the face, and then gather the information into a descriptor. Among these methods are Local Feature Analysis (LFA) [16], Gabor features [17], Elastic Bunch Graph Matching (EBGM) [18], and Local Binary Pattern (LBP) [19]. The last one is an extension of the LBP feature applied to the face recognition problem, which was originally designed as a texture descriptor [20]. LBP achieves better performance than previous methods; thus it is widely used nowadays. Newer methods, however, tried to overcome the shortcomings of LBP. One of them is the Local Directional Pattern (LDP) introduced by Jabid et al. [21, 22]. Furthermore, Zhang et al. explored the use of higher order derivatives to produce better results than LBP [23]. Both methods use other information than intensity to overcome noise and illumination variation problems. However, these methods still suffer in non-monotonic illumination variation, random noise, and change in pose, age, and expression condition. Although some methods, like Gradientfaces [24], have a high discrimination power under illumination variation, they still have low recognition capabilities for expression and age variation conditions.

In this paper, we propose a novel face descriptor, Local Gaussian Structural Pattern (LGSP), for robust face recognition that encodes the structural information, and the intensity variations of the face's texture. LGSP encodes the structural information in a local neighborhood, from eight different directions, using derivative-Gaussian compass mask. Consequently this mechanism is consistent against noise, since the edge response is more stable than intensity, and the derivative-Gaussian mask is robust against noise and illumination changes [24]. Then, from all the directions, we extract the absolute value of the eight directions' responses, and then we choose the top k maximum responses to create the code. Additionally, we compute a feature vector that comprises the histograms of directional features of different regions in the face. This approach allows us to distinguish the prominent directions of the edge responses and the variation of intensity changes. Furthermore, our descriptor uses the information of the entire neighborhood, instead of using sparse points for its computation like LBP. Hence, our approach conveys more information into the code.

The remaining of the paper is organized as follows. In Sections 2 and 3, we present a brief description of the LBP and LDP approaches. Section 4 introduces our method and describes the encoding scheme in detail. We present the analysis and the results of our method under expression, age, pose and illumination conditions in Section 5. Finally, we present concluding remarks in Section 6.

2. **LBP.**

The LBP operator, a gray scale invariant texture primitive, has gained significant popularity for describing the texture of an image [25]. It labels each pixel of an image by thresholding its P-neighbor values with the center value of the neighborhood, and converts the results into a binary number as shown in the following equation:

$$\mathrm{LBP}_{P,R}(x_c, y_c) = \sum_{p=0}^{P-1} \mathrm{s}(h_p - h_c)2^p, \tag{1}$$

$$s(x) = \begin{cases} 1, & \text{if } x \geq 0 \\ 0, & \text{if } x < 0 \end{cases}, \tag{2}$$

where h_c denotes the gray value of the center pixel (x_c, y_c), h_p corresponds to the gray values of P equally spaced pixels on the circumference of radius R at the center pixel, and $s(\cdot)$ is a function that assigns one to the positive arguments, otherwise it assigns zero. The values of the neighbors which do not fall exactly on a pixel position are estimated by bi-linear interpolation. In practice, the LBP computation (1) means that the signs of the differences in a neighborhood are interpreted as a P-bit binary number, resulting into 2^P distinct values for the binary pattern. These individual pattern values are capable of describing the texture information at the center pixel (x_c, y_c). The process of generating this P-bit pattern is shown in Figure 1.

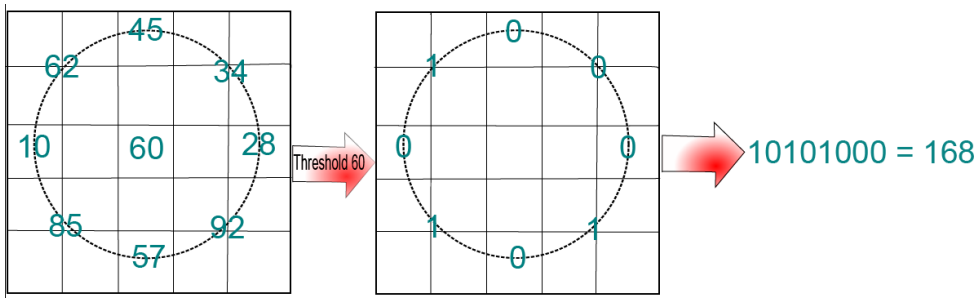

FIGURE 1. Basic LBP operator: P neighbors at R distance are used to compute the $\text{LBP}_{P,R}$ code.

Additionally, one variation of the original LBP, known as uniform LBP, is proposed from the observation that certain LBP codes appear more frequently in a significant image area. These patterns are considered uniform because they contain few transitions from one to zero or vice versa in a circular bit sequence. For example, the patterns 11111111 and 00000000 have zero transitions, while 00110000 has two transitions, and 10110001 has four transitions. Shan et al. [26] used this variant of the LBP, which has two transitions (LBP^{u_2}), for their facial recognition tasks. Though uniform LBP shows good recognition accuracy in a constraint environment, it is sensitive to random noise and non-monotonic illumination variation.

3. **LDP.** On the other hand, LDP computes the edge response values at different directions, and uses these responses to encode the image's texture. Since the edge response is less sensitive to illumination and noise than intensity, the resultant LDP feature describes the local primitives, including different types of curves, corners, and junctions, in a more stable manner, and also retains more information.

Therefore, LDP descriptor assigns an eight-bit binary code to each pixel of the input image. This pattern is then calculated by comparing the relative edge response values of a pixel in different directions. Given a central pixel in the image, the eight directional edge response values $\{m_i \mid i = 0, 1, \ldots, 7\}$, are computed using a Kirsch mask of size 3×3. Note that the response values are not equally important in all directions. Consequently, the presence of a corner or an edge shows high response values in some particular directions. Therefore, the LDP descriptor encodes the most prominent k directions to generate the code. Here, the top-k directional bit response are set to one, and the remaining $(8-k)$-bits

of the eight bit LDP pattern are set to zero. Hence, the LDP code is computed by:

$$\mathrm{LDP}_k(x_c, y_c) = \sum_{s=0}^{7} \mathrm{g}_k(|m_s|)2^s, \tag{3}$$

$$\mathrm{g}_k(x) = \begin{cases} 1, & \text{if } x \in \max_k\{m_i | i = 0, \ldots, 7\} \\ 0, & \text{otherwise} \end{cases}, \tag{4}$$

where m_s is the sth edge response for the center pixel (x_c, y_c), $\mathrm{g}_k(x)$ is a function that assigns one if the argument is in the k-top magnitudes of the center pixel, otherwise it assigns zero, and $\max_k$ returns the set of the top kth elements in the set. Figure 2 illustrates the mask response and LDP bit positions.

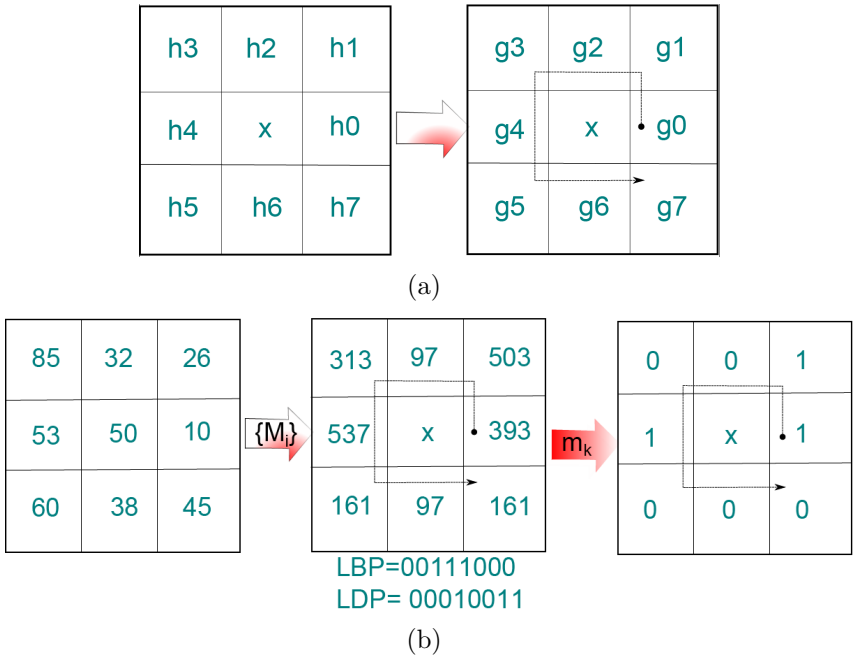

FIGURE 2. (a) Eight-directional edge response positions and the LDP binary positions and (b) LDP code computation using $k = 3$

4. **Local Gaussian Structural Pattern.** We propose a Local Gaussian Structural Pattern (LGSP) which is an eight-bit binary code assigned to each pixel of an input image that represents the texture's structure and its intensity transitions. As previous research [27, 28] showed, edge magnitudes are largely insensitive to lighting changes. Hence, we create the pattern by computing the edge response of the neighborhood using a derivative-Gaussian compass mask, and by conveying the absolutes values of the responses we build the code scheme, which represents the texture information of the picture. Moreover, we take the top k maximum directions of those edge responses to encode the dominant characteristics of the neighborhood.

One major problem of LBP [19] is the sparse sample that it uses to encode the neighborhood intensity changes. The few number of pixels used reduces the accuracy, discards most of the information in the neighborhood, and it makes the method sensible to noise and illumination changes. Moreover, these drawbacks are more evident for bigger neighborhoods. Hence, to avoid these problems all the neighborhood's pixels can be used, as LDP [21] does. Although the use of more information makes LDP stable, it recovers the

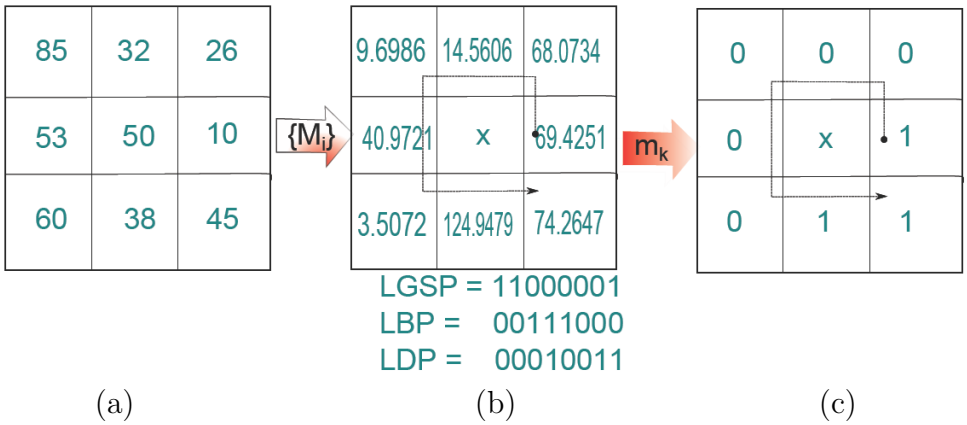

FIGURE 3. LGSP code computation. (a) A neighborhood with gray values, and (b) the derivative-Gaussian compass mask is applied to that neighborhood to extract the edge responses. From those responses, we choose the top three maximum directions to encode the texture in the neighborhood, and we marked the (c) LGSP binary positions that conveys the top three maximum responses.

information from the neighborhood using a mask that is limited in its search space, which reduces its resilience to noise and illumination. To avoid these problems we are proposing to use a derivative-Gaussian compass mask to compute the maximum responses of the neighborhood, to avoid the noise perturbation, and to make our method robust against illumination changes – as previous research [24] showed that the derivative of Gaussian is robust against these problems. Considering this process, we can recover more important information than the other state-of-the-art methods.

As Figure 3 shows, the top k maximum responses provide valuable information of the neighborhood's structure, e.g., lines, corners, and branches. However, the structural information is as reliable as its source. Hence, we need a stable mask to produce reliable edge information. Moreover, the use of a single neighborhood size discards useful information, as some descriptive features are visible only at different scales. Although Kirsch mask has been used widely, it lacks ability to represent the edge response in larger neighborhoods. Thereby, there is a need of a mask that can produce reliable edge responses regardless of the neighborhood size, noise, and illumination variation. Hence, our proposed mask fills this void, and incorporates information into the code consistently. Thus, our generated code is more robust against noise and illumination conditions, and can acquire more information from the face at different scales (as shown in Figure 4), that otherwise may be overlooked. Note that most methods do not have an increment in the encoded information as the size of the neighborhood increases – we discuss this behavior in Section 5.2. Furthermore, as previous research showed [29], it is vital to provide descriptive features for long range pixel interaction. However, neither LBP nor LDP consistently encode the long range pixel. We find that by combining the local shape information, the relation between the edge responses, the derivative-Gaussian compass mask, and the top k values of the maximum responses of the eight directions, we can better characterize the face's appearance.

4.1. **Compass mask.** Inspired by Kirsch mask [30], we use the derivative of a skewed Gaussian to create an asymmetric compass mask that we use to compute the edge response on the smoothed face. This mask is robust against noise and illumination changes, while producing strong edge responses on the image's texture. Hence, given a Gaussian mask

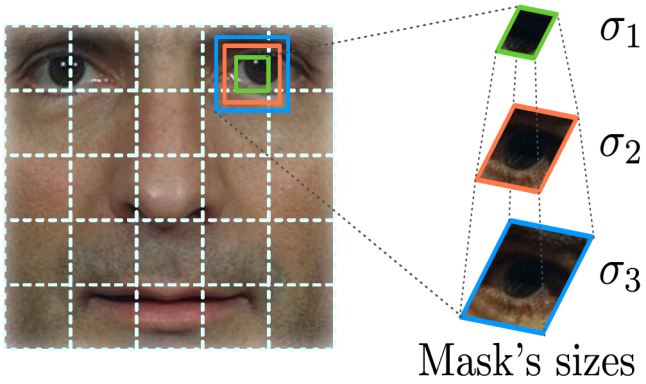

FIGURE 4. At different scales the derivative-Gaussian mask recovers distinctive features, that may be ignored by a single scale

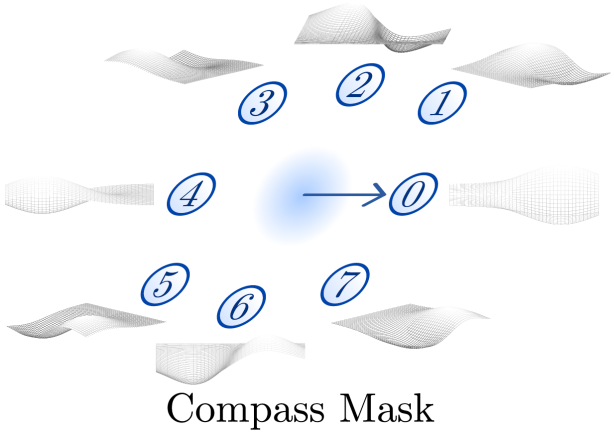

FIGURE 5. Rotated derivative-Gaussian compass masks

defined by:

$$G_\sigma(x,y) = \frac{1}{2\pi\sigma^2}\exp\left(-\frac{x^2+y^2}{2\sigma^2}\right), \tag{5}$$

where x, y are pixel location positions, and σ (sigma) is the width of the Gaussian bell; we define our mask as:

$$N_\sigma(x,y) = G'_\sigma(x+c,y) * G_\sigma(x,y), \tag{6}$$

where G'_σ is the derivative of G_σ with respect to x, σ (sigma) is the width of the Gaussian bell, $*$ represents the convolution operation, and c represents the offset of the Gaussian with respect to its center (in our experiments we use one fourth of the mask diameter for this offset). Then we generate a compass mask, $\{N^0_\sigma\text{-}N^7_\sigma\}$, by rotating N_σ 45 degrees apart, in eight different directions. Thus, we obtain a set of masks as shown Figure 5. Due to the rotation of the mask N_σ, we do not need to compute the derivative with respect to y of equivalent rotated masks.

However, our compass mask is capable of extracting important features of the face, such as facial shapes and facial objects, e.g., nose, mouth, eyes, and eyebrows, even under extreme lighting variations, which are key features for face recognition. Moreover, the mask reduces the effect of shadows, and it is robust against noise and illumination changes.

4.2. **Coding scheme.** In our coding scheme, we generate the code, LGSP_σ, by analyzing the edge response of each mask, $\{N^0_\sigma\text{-}N^7_\sigma\}$, that represents the edge significance in its

respective direction. Hence, to encode the information we used the top k maximum responses, which represent the most significant bits in the code, as show in Figure 3. Therefore, we define the code by:

$$\mathrm{LGSP}_\sigma = \sum_{j=1}^{k} 2^{Z_j^\sigma(x_c,y_c)}, \tag{7}$$

where (x_c, y_c) is the central pixel of the neighborhood being coded, Z_j^σ represent the maximum jth direction, which we define by:

$$Z_j^\sigma(x_c, y_c) = \arg\max_i{}_j\{N_\sigma^i(x_c, y_c) \mid 0 \le i \le 7\}, \tag{8}$$

where $\arg\max_j$ gives the jth maximum argument i, and N_σ^i represent the response of the ith direction.

4.3. **Face descriptor.** Each face is represented by an LGSP histogram (TH) as shown in Figure 6. The TH contains fine to coarse information of an image, such as corners, edges, spots and other local texture features. Given that the histograms only encode the occurrence of certain micro-patterns without location information, in order to aggregate the location information of the descriptor, we divide the face image into small regions, $\{R^1, \ldots, R^N\}$, and extract a histogram for each region. Finally, we compute the TH by concatenating each histogram by:

$$\mathrm{TH} = \prod_{i=1}^{N} \mathrm{H}^i, \tag{9}$$

where $\prod$ represents the concatenation operation, N is the number of the regions of divided face and H is the histogram of the ith region of the divided face. The spatially combined TH plays the role of a global face feature for the given face.

Consequently, TH is used during the face recognition process. The objective is to compare the encoded feature vector from one person with all other candidate's feature vector with the Chi-Square dissimilarity measure. This measure between two LGSP histograms, TH^1 and TH^2, is defined by:

$$\chi^2\left(\mathrm{TH}^1, \mathrm{TH}^2\right) = \frac{(\mathrm{TH}^1 - \mathrm{TH}^2)^2}{\mathrm{TH}^1 + \mathrm{TH}^2}, \tag{10}$$

the corresponding face of the feature vector with the lowest measured value indicates the match found.

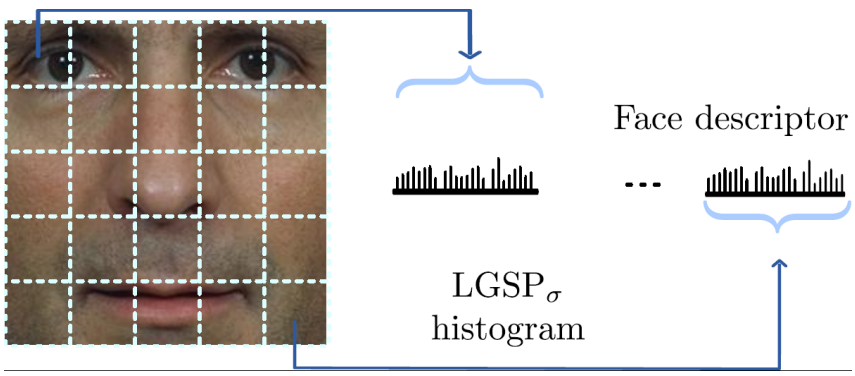

FIGURE 6. Face descriptor of the concatenated histograms of LGSP features

5. **Experiment and Results.** We perform four experiments to evaluate the performance of the proposed algorithm under, age, pose, illumination, and expression variation. We test our method in two different data sets: FERET and Yale B. Moreover, we cropped and normalized all the images to 100×100 pixels, based on the ground truth positions of the two eyes and mouth. In our experiments, every image is partitioned into a grid of 10×10 and 14×14, and we also test our method using the top two, three, and four maximum responses, to create the code scheme to each combination, and to prove the robustness of the proposed method. And for each set of maximum responses, we make the comparison with other state-of-the-art methods. These methods are the local encoding schemes: Local Binary Pattern (LBP) [19] and Local Directional Pattern (LDP) [21]. We also test the illumination robustness of the proposed method against another state-of-the-art methods: Gradientfaces [24], multiscale retinex (MSR) [31], self-quotient image (SQI) [32, 33] and, total variation model (LTV) [34].

5.1. **Data sets.** We test the performance of the methods, for face recognition problem, in accordance to use the CSU Face Identification Evaluation System with images from the FERET [35] database. We used *fa* image set as a gallery image and the other four sets as probe images: *fb*, for expression variation, *fc* for illumination variation, *dupI* and *dupII* for age variation.

Furthermore, we use the Yale B [36] database for illumination variation evaluation. It contains images of ten subjects with nine poses and 64 illuminations per pose. And we use the frontal face images of all subjects, each with 64 different illuminations. The faces are divided into five subsets based on the angle of the light source directions. The five subsets are: *sub1* (0° to 12°), *sub2* (13° to 25°), *sub3* (26° to 50°), *sub4* (51° to 77°), *sub5* (above 78°). We use *sub1* image set as a gallery image and other four sets as probe images.

5.2. **Neighborhood's size.** The increment in the neighborhood size increases the input data to the code. However, this data increment not necessarily will lead to incorporating more information into the code. Consequently, we analyze the impact of different mask sizes for the face recognition problem, and we show the results of this analysis in Figure 7. For the proposed method, we use different sizes of the derivative-Gaussian mask that depends on the given width value, σ (sigma), as shown in Figure 4. Therefore, we use a different σ (sigma), which approximately has the width of the desire neighborhood. For LBP, we change the radius of the neighborhood it uses. And for LDP, we test different ways of increasing its mask, because Jabid et al. only proposed a 3×3 mask, and we choose the one that gives best results. Thus, we increased the mask used in LDP by reproducing the zeros sums over the outer rings of the neighborhood, while maintaining the asymmetry of one side. The experiment revealed that our method is capable of differentiating more facial characteristics as the size of the derivative-Gaussian compass mask increases. However, this behavior is not present in the other methods, which have a lower recognition rate as the size of the neighborhood increases. The average results of the size variation of the neighborhoods, in the FERET database, are shown in Figure 7.

In our method, LGSP_σ, we use different sizes for the derivative-Gaussian compass mask to recover different characteristics of the face at those resolutions. However, this information is useful due to the encoding scheme proposed, while the other methods accuracy drops significantly. As Figure 7 shows, the average accuracy of LBP and LDP quickly drops as the size of the neighborhood increases. However, LGSP maintains the accuracy throughout the size increment. In the case of LBP, because it takes sparse points from the neighborhood, when the neighborhood's size increases these sparse points do not necessarily reflect the texture of such regions; thus reducing its average accuracy.

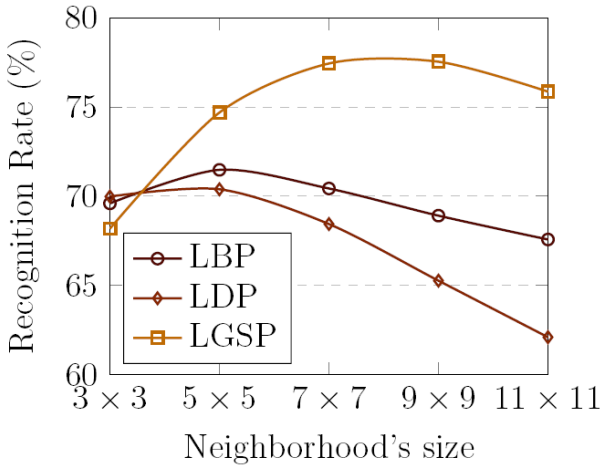

FIGURE 7. Average recognition rate on the FERET database for different neighborhood's sizes. The average accuracy of the other methods decreases as the size of their neighborhood increases. However, the proposed method has more stable response, as it can build a more discriminant structure for the large neighborhoods.

And for LDP, although it peaks at 5×5 neighborhood, in general, the method presents a drop in accuracy as the neighborhood size increases. Then, for larger neighborhoods it cannot distinguish textures with similar structures. However, LGSP takes advantage of the derivative-Gaussian mask to produce more reliable and stable code, regardless of the neighborhood's size. Therefore, in general the increment in the mask does not assure more discrimination power, if that information is not well used.

5.3. **Results on FERET database.** To evaluate the pose, age and expression variation robustness of our method, we perform the evaluation in the FERET [35] database. First, we evaluate the performance of the LGSP_σ code for single σ (sigma). In Figure 8 we show the variation of the recognition rate for different σ (sigma) values, and test our proposed method using the top two, three, and four responses with different grid's size.

The results for a single σ (sigma) (Figure 8) in age variation data sets (*dupI* and *dupII*) present an increment in the accuracy as the grid size increases, e.g., from 10×10 to 14×14, because each grid's cell conveys more discriminant information. In other words, as the grid's size increases the number of pixels in each cell decreases. Thus, the histogram of each cell would have fewer bins (as there are fewer possibilities in each cell), which lead to more discriminant histograms in the presence of a stable code (such as the proposed one). Furthermore, the results in the illumination variation data set (*fc*) also show this characteristic. However, the expression variation data set (*fb*) results have a decrement, in average, of 0.5%.

Figure 9, shows the comparison of LGSP with other two methods: LBP and LDP. Also, we explore the accuracy of Gradientfaces; however, due to its sub-par results in this database we do not show them here. Instead, see Section 5.6 for the discussion about this method. And Table 1 shows the comparison with others state-of-the-arts methods, as LBP, LDP (Kirsch), PCA, EBGM, and Bayesian. Although EBGM outperforms our method under expression variation by 3.46%, it decreases its recognition rate under illumination and age variation by more than 30%. Meanwhile, our method maintains the recognition rate in different environments, and in general, the results of our method outperform the results of the different state-of-the-art methods.

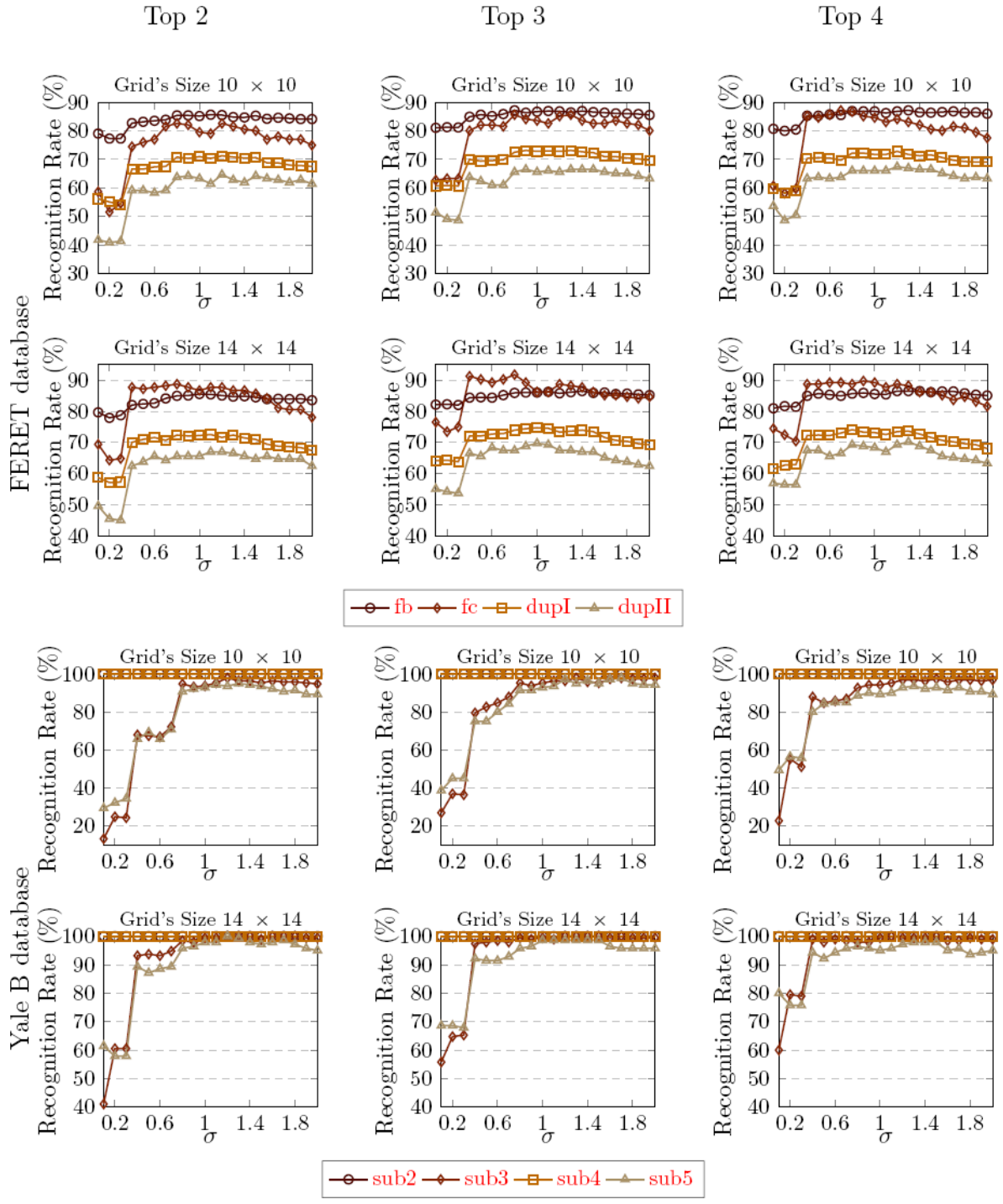

FIGURE 8. Recognition accuracy of LGSP_σ, with varying σ (sigma) in both databases, conveying the top two, three, and four maximum responses

5.4. **Robustness.** We made three more experiments to evaluate the robustness of the proposed method to the training data, and we compare against two methods: LBP and LDP. In our experiments, we change the training data set on FERET database, and test against the other data sets. Hence, in the first experiment, we use the data set *fb* as the training data set, and the rest for testing (*fa*, *dupI*, and *dupII*). The other two experiments, proceed in the same manner, and we use *dupI* and *dupII* as training data – Figure 10 shows the results of these experiments. The main idea behind these experiments, is to

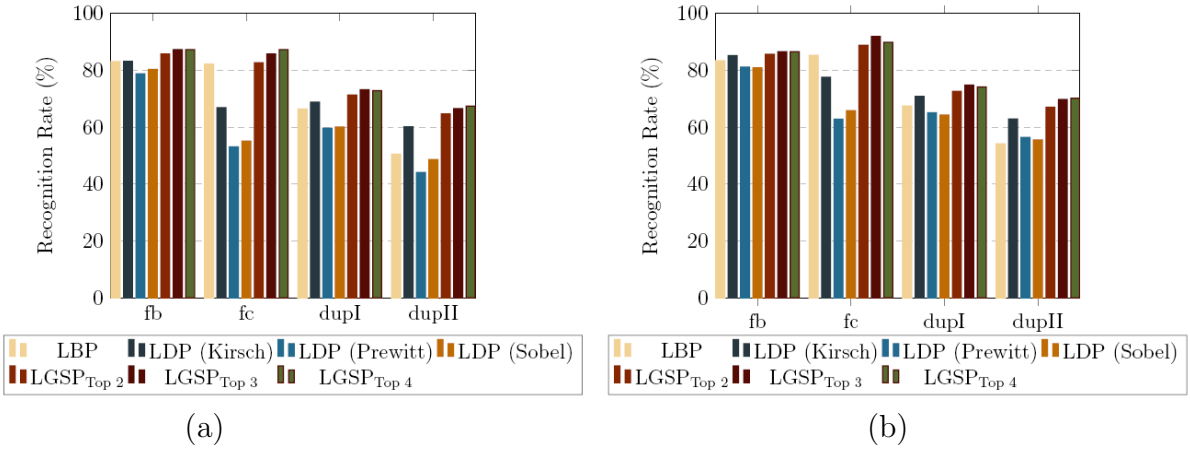

FIGURE 9. Comparison of the recognition rate of LGSP and state-of-the-art methods in the FERET database, with a grid size (a) 10×10 and (b) 14×14

TABLE 1. Performance comparison on FERET database for different methods

Subset	fb (%)	fc (%)	dupI (%)	dupII (%)
LBP	83.23	85.20	67.40	54.13
LDP (Kirsch)	85.12	77.55	70.83	62.84
PCA	85.00	65.00	44.00	22.00
EBGM	90.00	42.00	46.00	24.00
Bayesian	82.00	37.00	52.00	32.00
$\text{LGSP}_{\text{Top 3}}$	86.54	91.84	74.73	69.73

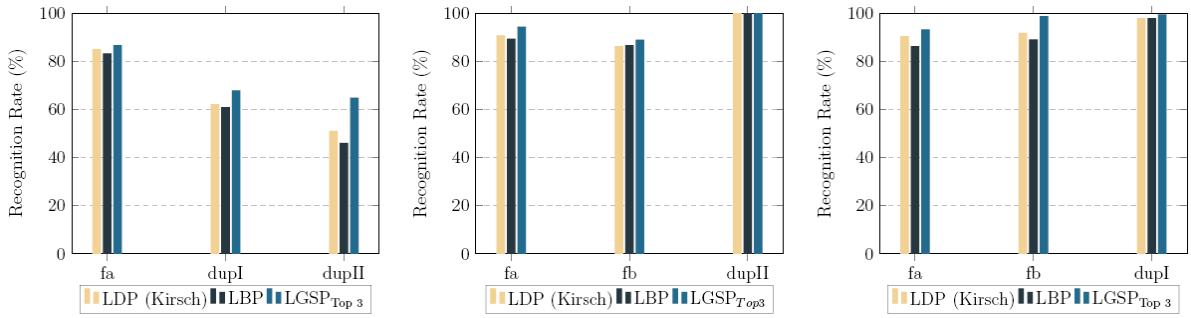

FIGURE 10. Comparison of the recognition rate of LGSP and state-of-the-art methods in the FERET database, with grid size 10×10, using (a) *fb*, (b) *dupI* and (c) *dupII* as training data

evaluate the independence of training data in the results. Therefore using PCA we can reduce the number of bins in the histogram and decrease the computational time.

5.5. **Noise evaluation.** To evaluate the robustness of the proposed method against noise, we corrupted the probe face images, using FERET database, with white Gaussian noise, and then try to identify them using the same process as described in Section 5. We perform this experiment with different levels of noise, and the results are shown in Figure 11. The robustness of LGSP, against noise, is notorious as it outperforms the other methods for every level of noise in every data set. LDP and LBP have problems

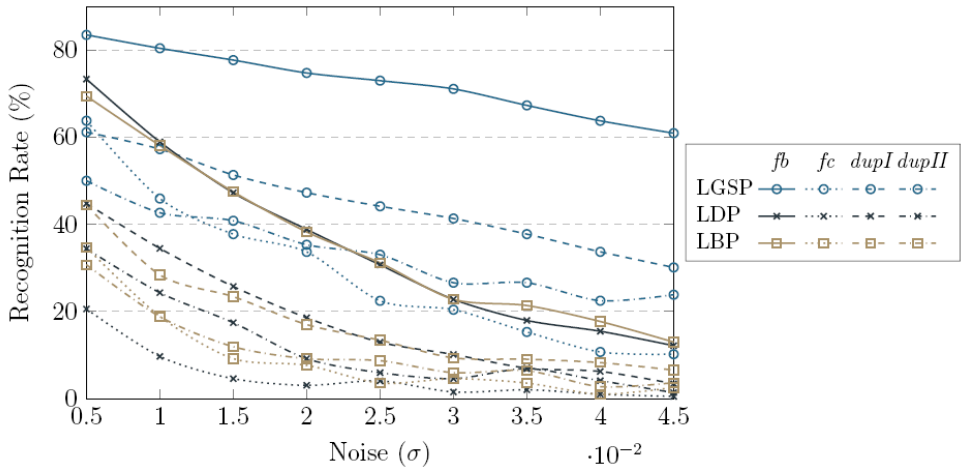

FIGURE 11. Recognition accuracy in the FERET database in presence of noise

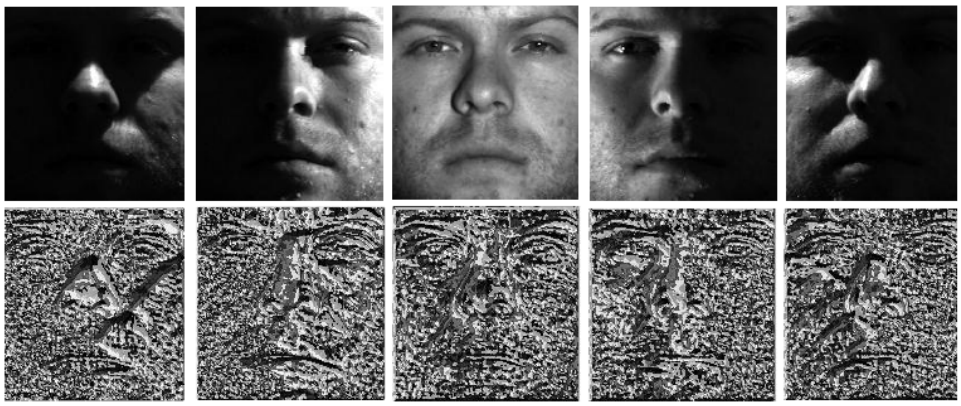

FIGURE 12. (Top row) Sample images of a single subject of the Yale B database under illumination variation, with the facial characteristics hidden by the shadows, (bottom row) and the LGSP coded faces, in which the facial features can be easily distinguished

overcoming the errors introduced by the noise. However, LGSP, due to its mask, has a highest recognition rate. The tendency of the results of Section 5.3 appears in the Figure 11 too. These results also show that the age variation is more challenging than expression and illumination variation. Nevertheless, LGSP scheme produces better results than other methods. Moreover, each LGSP scheme has different characteristics that can be exploited in certain conditions.

5.6. **Results on Yale B database.** We use the Yale B [36] database to evaluate the robustness of our method against illumination variation. The difficulty of this database increases for the subsets four and five, due to the illumination angles that cover half of the face with shadows. Nevertheless, our method is able to recover face features in the dark areas, as it does not rely on intensity like LBP. Figure 12 shows some samples faces and their respective LGSP coded face, and this demonstrates the capabilities of the method to recover characteristics in extreme illumination conditions. As the figure shows, the shadow in the face makes impossible to distinguish one eye and part of mouth. However, in the LGSP coded face eyes and the mouth can readily be identified. Moreover, the recognition accuracy in the subset four and five shows that our method outperforms the other ten methods using different grid sizes, 10×10 and 14×14.

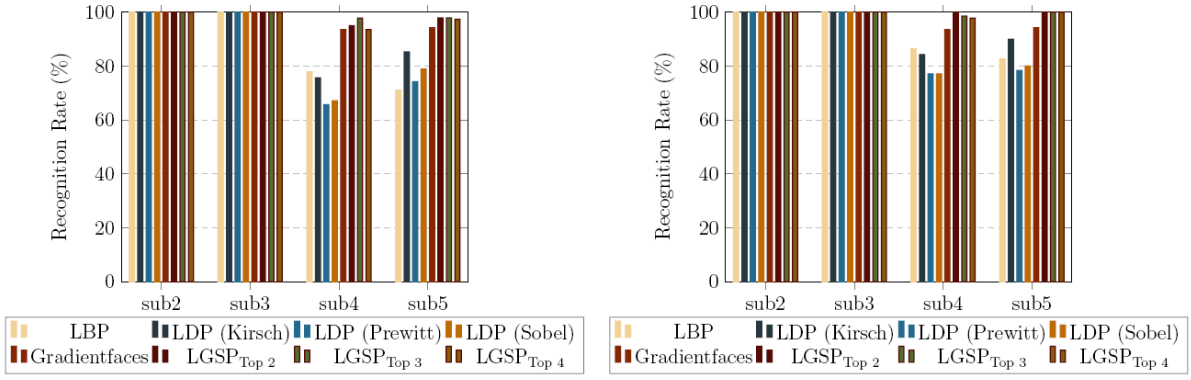

(a) (b)

FIGURE 13. Comparison of the recognition rate of LGSP and state-of-the-art methods in the Yale B database, with a grid size (a) 10×10 and (b) 14×14

TABLE 2. Performance comparison on the Yale B database

Subset	#2 (%)	#3 (%)	#4 (%)	#5 (%)
LBP	100.00	100.00	86.4286	82.6316
LDP (Kirsch)	100.00	100.00	84.4286	90.00
MSR	100.00	91.67	65	77.37
LTV	100.00	100.00	98.57	100.00
SQI	99.17	96.67	80.71	84.74
Harmonic images	100.00	99.70	96.90	n/a
Cones-attached	100.00	100.00	91.40	n/a
Cones-cast	100.00	100.00	100.00	n/a
Linear subspace	100.00	100.00	85.00	n/a
Gradientfaces	100.00	100.00	93.57	94.2105
$\text{LGSP}_{\text{Top2}}$	100.00	100.00	100.00	100.00

We evaluate our method against ten other methods. The comparison against similar methods, such as, LDP with different masks, LBP, and Gradientfaces, is shown in Figure 13. Table 2 shows a more general evaluation against other methods, e.g., MSR, SQR, LTV, Linear subspace [36], Cones-attached [36], Cones-cast [36], and Harmonic images [37]. All methods are flawless in the first two data sets, which have minor illumination changes. However, for the last two sets the recognition rate of the other methods decreases significantly. Specially, in the subset five, some methods are not capable of recognizing the face in these conditions. Moreover, LGSP is more robust than the other methods (at two different grid sizes), with all the different coding schemes (top two, three, and four). However, the Cones-cast method needs complicated 3-D model; thus, it cannot be applied in practical application. Moreover, the recognition rates on the subset five are not given.

6. **Conclusions.** In this paper we introduced a novel encoding scheme, LGSP that takes advantage of the structure of the face's textures and that encodes them efficiently. LGSP uses the directional information that is more stable against noise than intensity, to code the different patterns from the face's textures. Additionally, we introduced a derivative-Gaussian compass mask to extract this directional information. This mask is more stable against noise and illumination variation, which makes LGSP a reliable and stable coding

scheme. The code scheme that we presented, inherently, uses the absolute values of the neighborhoods and conveys the k maximum responses of the directions which allows it to distinguish similar texture's structures.

Furthermore, we evaluated LGSP under expression age and illumination variations, and found that it is reliable and robust throughout all these conditions, unlike other methods. For example, Gradientfaces had excellent results under illumination variation but failed with expression and age variations. However, LGSP is more robust under challenging illumination conditions. Also, LBP and LDP recognition rate deteriorates faster than LGSP in presence of noise and illumination changes.

Acknowledgment. This work was supported by the National Research Foundation of Korea (NRF) grant funded by the Korea government (MEST) (No. 2012-0005523).

REFERENCES

[1] P. J. P. W. Zhao, R. Chellappa and A. Rosenfeld, Face recognition: A literature survey, *ACM Comput. Surv.*, vol.34, no.4, pp.399-485, 2003.

[2] L. Sirovich and M. Kirby, Low dimensional procedure for the characterization of human faces, *J. Opt. Soc. Amer.*, vol.4, no.3, pp.71-86, 1987.

[3] M. Turk and A. Pentland, Eigenfaces for recognition, *J. Cognitive Neuroscience*, vol.3, pp.71-86, 1991.

[4] P. Belhumeur, J. Hespanha and D. Kriegman, Eigenfaces vs. fisherfaces: Recognition using class specific linear projection, *IEEE Transactions on Pattern Analysis and Machine Intelligence*, vol.19, pp.711-720, 1997.

[5] X. He, S. Yan, Y. Hu, P. Niyogi and H.-J. Zhang, Face recognition using laplacianfaces, *IEEE Transactions on Pattern Analysis and Machine Intelligence*, vol.27, pp.328-340, 2005.

[6] Y. Pang, Y. Yuan and X. Li, Iterative subspace analysis based on feature line distance, *Image Processing, IEEE Transactions on*, vol.18, pp.903-907, 2009.

[7] S. Lawrence, C. Giles, A. C. Tsoi and A. Back, Face recognition: A convolutional neural-network approach, *Neural Networks, IEEE Transactions on*, vol.8, pp.98-113, 1997.

[8] Z. H. Z. X. Tan, S. Chen and F. Zhang, Recognizing partially occluded, expression variant faces from single training image per person with som and soft knn ensemble, *IEEE Trans. on Neural Netw.*, vol.16, no.4, pp.875-886, 2005.

[9] S. Yan, H. Wang, X. Tang and T. Huang, Exploring feature descritors for face recognition, *Acoustics, Speech and Signal Processing, IEEE International Conference on*, vol.1, pp.629-632, 2007.

[10] Q. Z. C. Zhou, X. Wei and B. Xiao, Image reconstruction for face recognition based on fast ica, *International Journal of Innovative Computing, Information and Control*, vol.4, no.7, pp.1723-1732, 2008.

[11] J. Yang, A. Frangi, J.-Y. Yang, D. Zhang and Z. Jin, Kpca plus lda: A complete kernel fisher discriminant framework for feature extraction and recognition, *IEEE Transactions on Pattern Analysis and Machine Intelligence*, vol.27, pp.230-244, 2005.

[12] I G. P. S. Wijaya, K. Uchimura and Z. Hu, Face recognition based on dominant frequency features and multiresolution metric, *International Journal of Innovative Computing, Information and Control*, vol.5, no.3, pp.641-651, 2009.

[13] Y. Zana and R. M. Cesar Jr., Face recognition based on polar frequency features, *ACM Trans. on Applied Perception*, vol.3, no.1, pp.62-82, 2006.

[14] M. A. Turk and A. P. Pentland, Face recognition using eigenfaces, *Proc. of the Computer Vision and Pattern Recognition*, pp.586-591, 1991.

[15] T. S. B. Heisele and T. Poggio, A component-based framework for face detection and identification, *Int. J. Comput. Vision*, vol.7, no.4, pp.167-181, 2007.

[16] P. Penev and J. Atick, Local feature analysis: A general statistical theory for object representation, *Network: Computation in Neural Systems*, vol.7, no.3, pp.477-500, 1996.

[17] D. Gabor, Theory of communication, *J. Inst. Elect. Eng.*, vol.93, no.3, pp.429-457, 1946.

[18] L. Wiskott, J.-M. Fellous, N. Kuiger and C. von der Malsburg, Face recognition by elastic bunch graph matching, *IEEE Transactions on Pattern Analysis and Machine Intelligence*, vol.19, pp.775-779, 1997.

[19] T. Ahonen, A. Hadid and M. Pietikainen, Face description with local binary patterns: Application to face recognition, *IEEE Transactions on Pattern Analysis and Machine Intelligence*, vol.28, pp.2037-2041, 2006.

[20] T. Ojala, M. Pietikinen and D. Harwood, A comparative study of texture measures with classification based on featured distributions, *Pattern Recognition*, vol.29, no.1, pp.51-59, 1996.

[21] T. Jabid, M. Kabir and O. Chae, Local directional pattern (ldp) for face recognition, *Consumer Electronics (ICCE), Digest of Technical Papers International Conference on*, pp.329-330, 2010.

[22] M. Kabir, T. Jabid and O. Chae, A local directional pattern variance (ldpv) based face descriptor for human facial expression recognition, *Advanced Video and Signal Based Surveillance, the 7th IEEE International Conference on*, pp.526-532, 2010.

[23] B. Zhang, Y. Gao, S. Zhao and J. Liu, Local derivative pattern versus local binary pattern: Face recognition with high-order local pattern descriptor, *Image Processing, IEEE Transactions on*, vol.19, pp.533-544, 2010.

[24] T. Zhang, Y. Y. Tang, B. Fang, Z. Shang and X. Liu, Face recognition under varying illumination using gradientfaces, *Image Processing, IEEE Transactions on*, vol.18, pp.2599-2606, 2009.

[25] H. Zhou, R. Wang and C. Wang, A novel extended local-binary-pattern operator for texture analysis, *Inf. Sci.*, vol.178, pp.4314-4325, 2008.

[26] S. G. C. Shan and P. McOwan, Robust facial expression recognition using local binary patterns, *Proc. of IEEE Int. Conf. Image Process.*, pp.914-917, 2005.

[27] P. B. H. Chen and D. Jacobs, In search of illumination invariants, *Proc. of IEEE Conference on Computer Vision and Pattern Recognition*, vol.1, pp.254-261, 2000.

[28] H. Ling, S. Soatto, N. Ramanathan and D. Jacobs, A study of face recognition as people age, *Computer Vision, IEEE 11th International Conference on*, pp.1-8, 2007.

[29] S. Liao, M. Law and A. Chung, Dominant local binary patterns for texture classification, *Image Processing, IEEE Transactions on*, vol.18, pp.1107-1118, 2009.

[30] R. A. Kirsch, Computer determination of the constituent structure of biological images, *Computers & Biomedical Research*, pp.315-328, 1970.

[31] D. Jobson, Z. Rahman and G. Woodell, A multiscale retinex for bridging the gap between color images and the human observation of scenes, *Image Processing, IEEE Transactions on*, vol.6, pp.965-976, 1997.

[32] H. Wang, S. Li and Y. Wang, Face recognition under varying lighting conditions using self quotient image, *Proc. of the 6th IEEE International Conference on Automatic Face and Gesture Recognition*, pp.819-824, 2004.

[33] H. Wang, S. Z. Li and Y. Wang, Generalized quotient image, *IEEE Conf. Computer Vision and Pattern Recognition*, pp.498-505, 2004.

[34] T. Chen, W. Yin, X. S. Zhou, D. Comaniciu and T. S. Huang, Total variation models for variable lighting face recognition, *IEEE Transactions on Pattern Analysis and Machine Intelligence*, vol.28, no.9, pp.1519-1524, 2006.

[35] P. Phillips, H. Moon, S. Rizvi and P. Rauss, The feret evaluation methodology for face-recognition algorithms, *IEEE Transactions on Pattern Analysis and Machine Intelligence*, vol.22, pp.1090-1104, 2000.

[36] A. Georghiades, P. Belhumeur and D. Kriegman, From few to many: Illumination cone models for face recognition under variable lighting and pose, *IEEE Transactions on Pattern Analysis and Machine Intelligence*, vol.23, pp.643-660, 2001.

[37] L. Zhang and D. Samaras, Face recognition under variable lighting using harmonic image exemplars, *Proc. of IEEE Computer Society Conference on Computer Vision and Pattern Recognition*, vol.1, pp.19-25, 2003.